Structural changes in profilin accompany its binding to phosphatidylinositol 4,5-bisphosphate

Vidya Raghunathan[a], Patrick Mowery[b], Michael Rozycki[a], Uno Lindberg[c] and Clarence Schutt[a]

[a]Frick Chemical Laboratory, Washington Road, Princeton University, Princeton, NJ 08544, USA, [b]American Cyanamid,
P.O. Box 400, Princeton, NJ 08543-0400, USA and [c]Zoological Cell Biology, WGI, Arrhenius Laboratories for Natural
Sciences, Stockholm University, S-10691 Stockholm, Sweden

The effect on the structure of profilin of phosphatidylinositol 4,5-bisphosphate (PIP₂) binding was probed by fluorescence and circular dichroism (CD) spectroscopy. Fluorescence of Trp^3 and Trp^{31} of profilin at 292 nm showed a linear decrease in solution emission at 340 nm as PIP₂/profilin was increased from 0 to 80:1, apparently due to a static quenching mechanism involving formation of a nonfluorescent PIP₂/profilin complex. CD spectra revealed an increase of up to 3.3-fold in the molar ellipticity at 222 nm for profilin as it binds PIP₂, as well as changes in the Cotton effect between 250 and 310 nm. These results are consistent with a possible increase in the α-helix content of profilin triggered by the binding of PIP₂.

Circular dichroism; Fluorescence; α-Helix; Phosphatidylinositol 4,5-bisphosphate; Profilin; Protein conformation

1. INTRODUCTION

Phosphatidylinositol 4,5-bisphosphate (PIP₂) and phosphatidylinositol 4-monophosphate (PIP) bind to profilin, disrupting its interaction with actin and leading to increased polymerization of free G-actin in vitro [1,2]. This interaction is specific at physiological salt concentrations (80 mM KCl, 10^{-6} M Ca^{2+}), whereas at lower ionic strength anionic phospholipids such as phosphatidic acid (PA) and phosphatidylinositol (PI) also bind to profilin [2]. The question arises whether PIP₂ binds to the profilin:actin complex with the subsequent release of free actin, or whether PIP₂ binds free profilin and induces the dissociation of actin from profilin by mass action [2,3]. Forthcoming high resolution structural information from crystals of profilin:actin [4] will elucidate the nature of the interaction between profilin and actin, but no information exists as yet about the possible effects of PIP₂ on the structure of either profilin or profilin:actin.

In this investigation, we present evidence from circular dichroism (CD) and fluorescence spectroscopy that the fluorescence of profilin is quenched by PIP₂ through a static mechanism involving the formation of a nonfluorescent groundstate complex. CD spectra show that the binding of PIP₂ to profilin is accompanied by an increase up to 3.3-fold in the molar ellipticity of profilin at 222 nm, and is compatible with an increase in the α-helical content of profilin from 5% to as much as 35%. Such structural changes in profilin may be im-

portant in triggering the dissociation of actin from profilin:actin.

2. MATERIALS AND METHODS

2.1. Sample preparation

PIP₂ was purified from an acid extract of fresh bovine brain [5] by affinity chromatography on a neomycin adduct column [6], and the purity of the lipid was determined by ^{31}P-NMR, thin layer chromatography [7] and phosphate analysis [8].

Profilin was purified from calf thymus profilin/actin prepared by poly(L-proline)-Sepharose affinity chromatography [9,10]. Profilin/actin was dissociated in 1 M potassium phosphate, pH 7.3, 3 mM $MgCl_2$, 5 mM ATP and 5 mM DTT; centrifuged for 2 h at 100 000 × g to pellet filamentous actin; and passed over a DEAE-Sephadex A-50 column [11]. The resulting pure profilin was concentrated in an Amicon ultrafiltration cell (YM-10 membrane) and dialyzed overnight against two changes of high salt buffer (HSB) consisting of 6 mM phosphate, pH 7.3; 140 mM KCl, 6 mM NaCl, 0.1 mM EGTA. Protein concentrations were determined by UV absorption at 280 nm using an $E_{280}^{1\%}$ of 1.2, or with a Coomassie blue binding assay (Bio-Rad, Richmond, CA, USA).

PIP₂ concentrations above the critical micelle concentration of 30 μM [6] were used in all experiments after sonication for 5 min in HSB using a W-385 Branson-type bath sonifier (Heat Systems, NY, USA). Samples were prepared by mixing appropriate proportions of sonicated PIP₂ and profilin and incubating for 1–2 h at 25°C, although varying the incubation times from 15 min to 8 h did not significantly affect the results.

2.2. Fluorescence spectroscopy

Fluorescence data was recorded at 25°C with an SLM 48000 spectrometer using a focused xenon lamp, MC200 excitation monochromator and an emission monochromator. Photomultipliers were cooled R28A's. Polarizers were set at the magic angle [12] to help correct for scattering artifacts. Emission spectra were acquired with a 2 nm slit-of-emission monochromator while exciting at 292 nm through 4 nm slits, and were corrected for photomultiplier response using values supplied by SLM. Fluorescence lifetimes were obtained by the multi-

frequency phase and modulation method using frequencies between 25 and 100 MHz [12], and data was analyzed using both the multiple exponential technique based on the Marquardt algorithm [13], as well as distributed lifetime analysis [14,15]. Excitation was at 292 nm, whereas emission was through a WG320 filter using light scattering as a reference. Distributed lifetimes were fit assuming a Lorentzian distribution. The goodness of fit (χ_i^2) was expressed as the error-weighted sum of the squared deviations between the model and data, and was minimized until all systematic errors could be removed from the model.

Fluorescence quenching was analyzed according to a variation of the Stern–Volmer equation [12]:

$$F_o/F = 1 + K_a [PIP_2] \qquad \text{Equation 1}$$

where F and F_o are the fluorescence of profilin in the presence and absence of quencher (PIP_2) and K_a is the quenching constant for the PIP_2 micelle and protein instead of the more familiar bimolecular quenching constant. F_o/F characterizes the relative change in fluorescence intensity accompanying the binding of profilin to PIP_2.

2.3. Circular dichroism spectroscopy

CD spectra were recorded with a Mark 5 spectrometer (Instruments SA, Metutchen, NJ, USA) in the ranges 200 to 260 nm and 250 to 300 nm using 17 μM profilin and varying concentrations of PIP_2 at room temperature. This concentration gave the optimal signal-to-noise ratio with low scattering from chloride ions and lipid. Since the spectrum at 222 nm is dominated by contributions from α-helices, the molar ellipticity ($[\theta]_{222}$) has been shown [16] to be related to the helical content of the protein, f_H:

$$[\theta]_{222} = -30,300 f_H - 2340 \qquad \text{Equation 2}$$

where $-30,300$ is the ellipticity of pure helix. PIP_2 at concentrations comparable to those used in the presence of profilin gave no measurable spectrum.

2.4. Gel filtration chromatography

Gel filtration chromatography was carried out on a Pharmacia (Uppsala, Sweden) Superose-12 HR10/30 column in HSB at 4°C and a flow rate of 0.25 ml·min^{-1}.

3. RESULTS

3.1. Fluorescence spectroscopy

Profilin has two N-terminal tryptophan residues at positions 3 and 31 whose combined steady-state fluorescence emission spectra with 292 nm excitation are maximal at 338 nm, suggesting a partially buried environment for these residues [17]. Fig. 1a shows that the addition of PIP_2 quenches the fluorescence of profilin with no accompanying wavelength change in the fluorescence maximum. A Stern–Volmer plot shows an increase in the relative fluorescence intensity F_o/F as a linear function of PIP_2 concentration (Fig. 1b), indicating that quenching by PIP_2 of the tryptophan fluorescence may arise from either dynamic quenching due to collisional interactions between PIP_2 and profilin, or static quenching arising from the formation of a non-fluorescent, ground-state complex [12].

Nonlinear least squares analysis of the data was used to obtain the frequency dependence of the fluorescence phase shift and demodulation for both free profilin and 40:1 PIP_2/profilin (Fig. 2a,b). A single component is
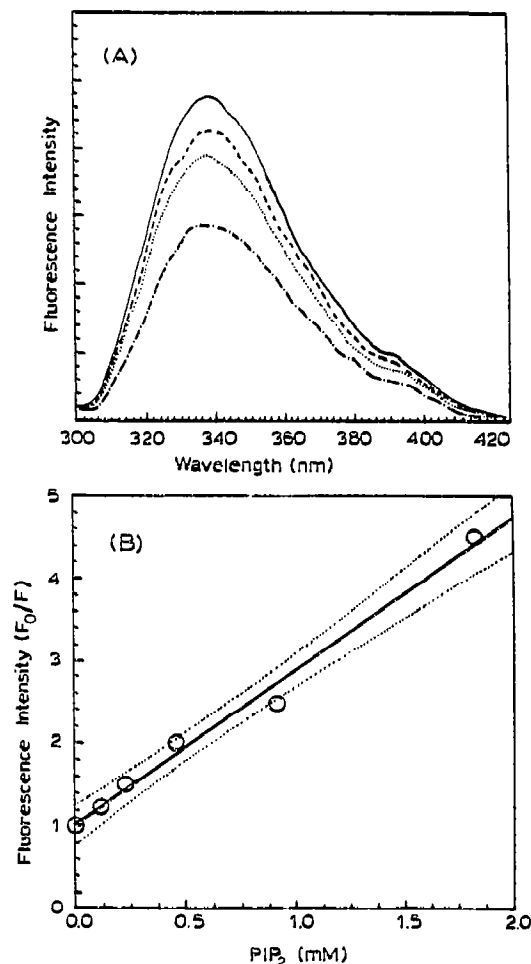

Fig. 1A. Tryptophan fluorescence emission spectra of profilin in the presence of PIP_2. Spectra were recorded with 17 μM profilin in HSB at PIP_2/Profilin ratios of 0:1 (———), 5:1 (— —), 10:1 (....) and 20:1 (-----). B. Stern–Volmer plot of relative fluorescence intensity as a function of PIP_2 concentration. Profilin at 23 μM was used at PIP_2:profilin ratios of 5:1, 10:1, 20:1, 40:1 and 80:1. The dotted lines represent the deviation of the measurement at a given PIP_2 concentration from the linear least squares fit of the data.

sufficient to model the tryptophan lifetimes at low PIP_2 concentrations. However, at higher PIP_2 concentrations, two exponentials are required (Table I), a principal component lifetime of 1.57 ± 0.03 ns and a minor component lifetime of 5.54 ± 0.11 ns, which is inconsistent with the single-component system implied by the linear dependence of fluorescence quenching on the concentration of PIP_2.

A clearer picture was obtained from distributed lifetime analysis of the intrinsic fluorescence lifetimes [14,15] (Fig. 2c). The data for profilin alone and at 40:1 PIP_2/profilin could be fit by a single Lorentzian with an average lifetime of 1.92 ns ($\chi_i^2 = 1.06$ and 1.02, respectively) as described in Table I. This analysis provided better support than the nonlinear least squares analysis
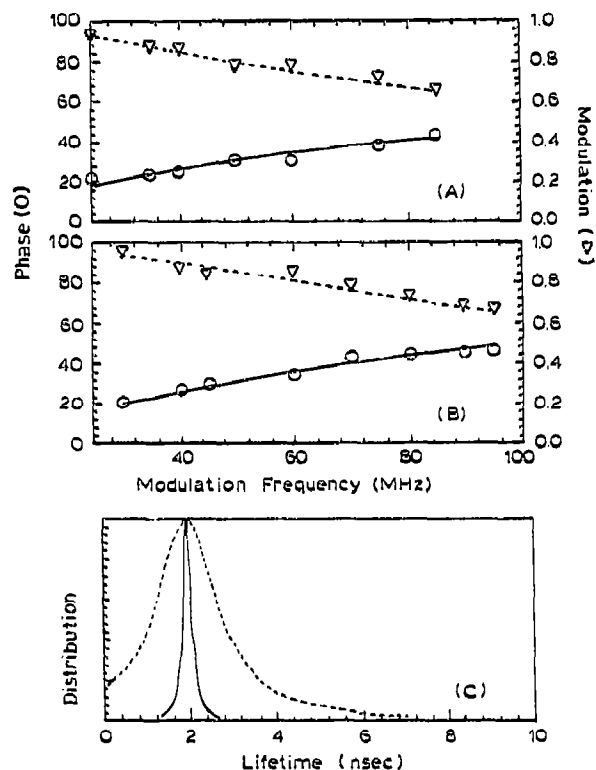
Fig. 2. Measurement of fluorescence lifetimes. Phase and demodulation are shown as circles and triangles respectively for (A) 40:1 PIP$_2$:profilin and (B) pure profilin. Samples were prepared as in Fig. 3. Modulation frequencies used were between 30 and 95 MHz for profilin and 25 to 85 MHz for 40:1 PIP$_2$/profilin. (C) Distributed lifetime fit of the data in (A) and (B). The solid line corresponds to profilin and the dotted line to the 40:1 PIP$_2$/profilin complex.

1b). The increase in the fluorescence lifetime peak width from 0.22 ns for profilin alone to 1.65 ns for 40;1 PIP$_2$/ profilin suggests an increase in the number of excited or ground-state conformations of profilin in the presence of PIP$_2$ [14,15,18].

3.2. Circular dichroism spectroscopy

CD spectra in the range from 200 to 250 nm were obtained for profilin in the presence of PIP$_2$ (Fig. 3). The high ionic strength of the solution and interference from PIP$_2$ limit useful spectral data to the region above 205 nm, where α-helix content is the only protein secondary structural information that can be obtained reliably [19]. Even at 208 nm, the expected position for one of the characteristic peaks arising from α-helices, the molar ellipticity of pure profilin (-2625 deg·cm^2·dmol^{-1}) is on the order of contributions expected from pure β-sheet and random coil [20] and cannot be used as a reliable measure of helicity.

Fig. 3a shows that $[\theta]_{222}$ for profilin in the absence of PIP$_2$ is -3872 deg·cm^2·dmol^{-1}, which from equation 2 corresponds to an α-helix content of approximately 5%. This is on the order of the 8–15% helix content previously described for profilin [11]. Fig. 3 shows that $[\theta]_{222}$ increases by 85%, from -3872 to -7159 deg·cm^2·dmol^{-1}, as PIP$_2$/profilin is increased from 0 to 20:1. In addition, a shoulder begins to emerge at 208 nm at the higher PIP$_2$ concentration. Since PIP$_2$ alone has no contribution to the CD spectrum in this region, these effects suggest that the α-helix content of profilin is increased by the addition of PIP$_2$ [16,20,21].

The total ellipticity of profilin in solution is the sum of the contributions from free profilin and profilin bound to PIP$_2$. Gel filtration chromatography [2,22] on Superose-12 was used to separate free and PIP$_2$-bound profilin. PIP$_2$/profilin elutes as a peak at 43% of the total column volume, followed by free profilin at 66%, and phosphate determination shows negligible contamination of free profilin by PIP$_2$. The dependence of the fractions of free and bound profilin on PIP$_2$ concentration is given in Table II. An independent measure of the proportions of bound and unbound profilin can be obtained using values of F_0/F from the Stern–Volmer treatment of PIP$_2$ binding to profilin (Fig. 1b), because the static quenching mechanism requires the PIP$_2$/pro-

for a one-component fit model, and hence better agreement with the observed linear quenching of profilin by PIP$_2$. Dynamic quenching requires that $F_0/F = \tau_0/\tau$, where τ_0 is the fluorescence lifetime of free profilin and τ is the profilin lifetime at a given PIP$_2$ concentration. Since the observed fluorescence lifetime of 1.92 ns is independent of the concentration of PIP$_2$, the quenching of profilin by PIP$_2$ follows a static mechanism whereby free profilin is the fluorescent species and PIP$_2$ binds profilin to form a non-fluorescent complex. This mechanism appears to hold for PIP$_2$/profilin up to 80:1 (Fig.

Table I

Fluorescence lifetime in nanoseconds of free and PIP$_2$-bound profilin determined by multi-frequency analysis. F_n corresponds to the fraction of the component with a lifetime of τ_{ii}. W refers to the width at half height for the distributed lifetime analysis in Fig. 2c.

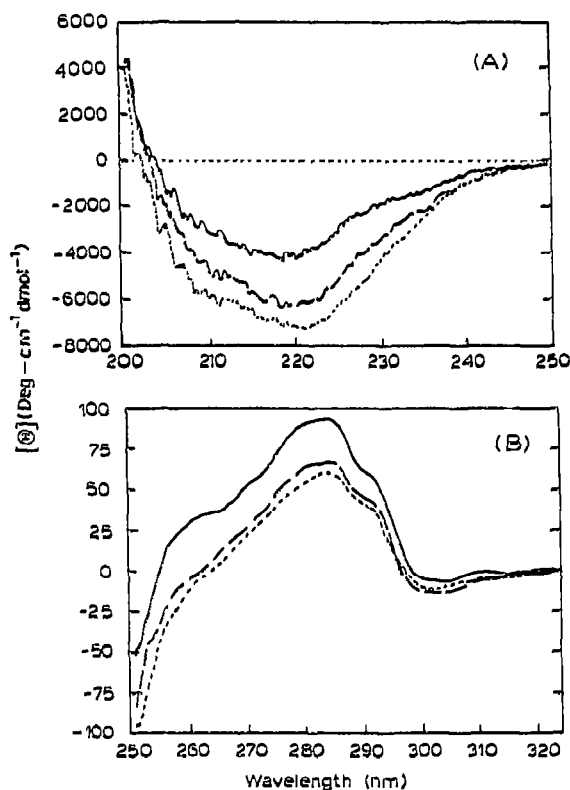| | Nonlinear least squares analysis | | | | | | | Distributed lifetime analysis | | | |
	One component			Two-component							
PIP$_2$/P	τ_1	F_1	χ_1^2	τ_1	τ_2	F_1	χ_1^2	τ	W	F_1	χ_1^2
0:1	1.92	1.0	1.24	1.86	3.36	0.96	1.4	1.92	0.22	1.0	1.06
40:1	2.05	1.0	1.5	1.54	5.54	0.8	1.1	1.92	1.65	1.0	1.02

Fig. 3. Circular dichroism spectra of 27.4 μM profilin in the presence of varying concentrations of PIP$_2$, corrected against HSB (see text). (A) 200–250 nm spectra at PIP$_2$/profilin ratios of 0:1 (——), 10:1 (— —), 20:1 (-----) and 1:0 (....). (B) 250–350 nm spectra at PIP$_2$/profilin 0:1 (——), 10:1 (— —) and 20:1 (-----) PIP$_2$/profilin.

filin complex to be totally quenched. Table III shows that $[\theta]_{222}$ for PIP$_2$-bound profilin increases 2.9- to 3.3-fold over that for profilin alone. The fraction of bound profilin at a given PIP$_2$/profilin ratio determined from fluorescence is slightly higher than that determined chromatographically, probably due to dissociation of PIP$_2$/profilin on the column, resulting in a lower apparent $[\theta]_{222}$ for PIP$_2$/profilin. Equation 2 gives an α-helix content for PIP$_2$/profilin of 29% to 35%.

CD spectra were also obtained in the region from 250 to 290 nm in which contributions from tertiary structure predominate (Fig. 3b). The most apparent change in this region is a decrease in the intensity of the Cotton

Table II

Quantitation of free and PIP$_2$-bound profilin (P) eluted from Superose-12 after incubation with PIP$_2$.

Total P (μM)	PIP$_2$/P	Free P (μM)	Bound P (μM)
23	(0:1)	23.0	0.0
23	(10:1)	17.3	5.7 (25%)
23	(20:1)	14.7	8.3 (36%)
23	(40:1)	10.1	12.9 (56%)

Table III

Calculation of the molar ellipticity of PIP$_2$/profilin using gel filtration (GF) and fluorescence (F) data.

Molar ellipticity of the PIP$_2$/profilin complex, $[\theta]_{222} = [\theta]_{222}{}^{F}\chi_{F} + [\theta]_{222}{}^{B}\chi_{B}$ where $[\theta]_{222}{}^{F}$ and $[\theta]_{222}{}^{B}$ are the molar ellipticities at 222 nm of free and bound profilin, respectively, and χ_{F} and χ_{B} represent the mole fraction of free and PIP$_2$-bound profilin; $\chi_{B} + \chi_{F} = 1$. PIP$_2$/P represents the complex. Each $[\theta]_{222}$ shown represents an average of 8 measurements between 222 ± 0.6 nm, and is given in units of (deg·cm^2·dmol^{-1}). Data is given for gel filtration (GF), and fluorescence data (F).

PIP$_2$/P	$-[\theta]_{222}$		χ_{B}	$-[\theta]_{222}$ PIP$_2$:P
0:1	3872		--	--
10:1	6086	GF	0.25	12,728
		F	0.31	11,014
20:1	7159	GF	0.36	13,002
		F	0.46	11,018

effect with increasing concentration of PIP$_2$, which is characteristic of a change in the environment of the tryptophans. The binding of PIP$_2$ may also affect tyrosine and phenylalanine residues in profilin as suggested by a loss of intensity between 260 and 280 nm. CD measurements on profilin in the presence of PIP show increasing molar ellipticity of profilin solutions in the same range of phospholipid concentrations as for PIP$_2$ (data not shown), whereas phosphatidic acid (PA) and phosphatidylinositol (PI) have no effect.

4. DISCUSSION

In this study we present evidence for a PIP$_2$-induced conformational change in profilin at salt concentrations which maximize the specificity of the PIP$_2$/profilin interaction [2]. Induction of secondary structure changes by PIP$_2$ binding has already been described for glycophorin, an intrinsic membrane protein [23], and for myelin basic protein, a protein with a very low native α-helix content [24].

Distributed lifetime analysis of profilin fluorescence quenching by PIP$_2$ indicates that the tryptophan residues at positions 3 and 31 are involved in the formation of a nonfluorescent complex with PIP$_2$, in accordance with a static quenching mechanism. The linearity of the Stern–Volmer plot up to 80:1 PIP$_2$/profilin suggests that both tryptophans are quenched equally by PIP$_2$. These observations are corroborated by CD spectra in the 250–290 nm region which suggest a change in the environment of the tryptophan residues. Circular dichroism spectroscopy of profilin in the absence of PIP$_2$ suggests that native profilin has a very low α-helix content, ranging from 5% as observed in this study to 8 to 15% [11]. PIP$_2$ binding increases the molar ellipticity of profilin, and equation 2 can be used to calculate an α-helix content of 29 to 35% for the PIP$_2$/profilin complex. This appears to be an unusually large change. The uncertainty in measuring low ellipticities probably renders insignificant the difference between a

calculated helix content of 5% and one of 15%, and the difficulty in modelling spectra that do not extend below 190 nm [19] may lead to an overestimation of the helicity in PIP$_2$/profilin. While an upper limit of 35% should be regarded cautiously for the α-helix content induced in profilin by PIP$_2$, there is no doubt concerning the qualitative significance of the increase.

Malm et al. [11] noted that their CD-based estimate of the helix content for profilin was considerably less than the 30% predicted from the amino acid sequence [25]. Furthermore, since their CD spectrum of profilin/ actin was similar to the superposed spectra for profilin and actin alone, they argued that the binding of profilin to actin was not accompanied by significant structural changes. PIP$_2$ binds to profilin in the micelle state at a stoichiometry of 7:1 to 10:1 [1,22], and if free profilin exists in a conformation possessing less secondary structure than predicted, the binding of a stoichiometric excess of PIP$_2$ could drive profilin through a structural transition disfavoring actin binding. Thus, PIP$_2$ may trigger the formation of an α-helix in profilin as it dissociates from actin.

Our results suggest a possible location for the induced α-helix formation in profilin in the region between Trp$_3$ and Trp$_{31}$, since fluorescence quenching implicates these residues in the formation of a nonfluorescent complex with PIP$_2$. The range of helicity induced in profilin by PIP$_2$ is consistent with a helix or helices of up to 30 residues, and the forthcoming x-ray crystal structure of profilin/actin [4] should contribute to an understanding of regions of profilin which could undergo helical transitions. PIP$_2$ has been found to mediate interactions between actin and both gelsolin [26], and CapZ [27], in each case regulating the subsequent polymerization of G-actin. It will be interesting to determine whether PIP$_2$-induced helical transitions are also a general characteristic of these actin-binding proteins.

REFERENCES

[1] Lassing, I. and Lindberg, U. (1985) Nature 314, 472–474.

[2] Lassing, I. and Lindberg, U. (1988) J. Cell. Biochem. 37, 255–267.

[3] Goldschmidt-Clermont, P.J., Machesky, L.M., Baldassare, J.J. and Pollard, T.D. (1990) Science 247, 1575–1578.

[4] Schutt, C.E., Lindberg, U., Myslik, J. and Strauss, N. (1989) J. Mol. Biol. 209, 735–746.

[5] Scacht, J. (1981) Methods Enzymol. 72, 626–631.

[6] Palmer, F.B.St.-C. (1981) Can. J. Biochem. 59, 469–476.

[7] Palmer, F.B.St.-C. (1981) J. Lipid Res. 22, 1296.

[8] Ames, B.N. and Dubin, D.T. (1960) J. Biol. Chem. 235, 769.

[9] Tanaka, M.H. and Shibata, H. (1985) Eur. J. Biochem. 151, 291–297.

[10] Lindberg, U., Schutt, C.E., Hellsten, E., Tjader, A.C. and Hult, T. (1988) Biochim. Biophys. Acta 987, 391–400.

[11] Malm, B., Larsson, H. and Lindberg, U. (1983) J. Musc. Res. Cell Mot. 4, 569–588.

[12] Lakowicz, J.R. (1986) Principles of Fluorescence Spectroscopy, Plenum Press, New York.

[13] Lakowicz, J.R., Laczko, G., Cherek, H., Gratton, E. and Limekman, M. (1984) Biophys. J. 46, 463–477.

[14] Alcala, J.R., Gratton, E. and Prendergast, F.G. (1987) Biophys. J. 51, 925–936.

[15] Alcala, J.R., Gratton, E. and Prendergast, F.G. (1987) Biophys. J. 51, 597–604.

[16] Chen, Y.H., Yang, J.T. and Martinez, H.M. (1972) Biochemistry 11, 4120–4131.

[17] Eftink, M.R. and Ghiron, C.A. (1976) Biochemistry 15, 672–680.

[18] Ross, J.B., Roussalang, K.W. and Brand, L. (1981) Biochemistry 20, 4361–4369.

[19] Johnson, W.C. (1990) Proteins 7, 205–214.

[20] Greenfield, N. and Fasman, G.F. (1969) Biochemistry 8, 4108–4116.

[21] Doty, P. and Yang, J.T. (1956) J. Am. Chem. Soc. 78, 498–500.

[22] Machesky, L.M., Goldschmidt-Clermont, P.J. and Pollard, T.D. (1990) Cell Reg. 1, 937–950.

[23] Verpoorte, J.A. and Palmer, F.B.St.-C. (1977) FEBS Lett. 84, 159–162.

[24] Anthony, J.S. and Moscarello, M.A. (1971) Biochim. Biophys Acta 243, 429–433.

[25] Nystrom, L.-E., Lindberg, U., Kendrick-Jones, J. and Jakes, R. (1979) FEBS Lett. 101, 161–165.

[26] Janmey, P.A. and Stossel, T.P. (1987) Nature 325, 362–364.

[27] Heiss, S.G. and Cooper, J.A. (1991) Biochemistry 30, 8753–8758.